Superconductor
Science and
Technology

PAPER

Modeling of *LC*-shunted intrinsic Josephson junctions in high-T_c superconductors

To cite this article: Yu M Shukrinov *et al* 2017 *Supercond. Sci. Technol.* **30** 024006

IOP Publishing Superconductor Science and Technology
Supercond. Sci. Technol. 30 (2017) 024006 (8pp) doi:10.1088/1361-6668/30/2/024006

Modeling of *LC*-shunted intrinsic Josephson junctions in high-T_c superconductors

Yu M Shukrinov[1,2], I R Rahmonov[1,3], K V Kulikov[1,2], A E Botha[4], A Plecenik[5], P Seidel[6] and W Nawrocki[7]

[1] BLTP, Joint Institute for Nuclear Research, Dubna, Moscow Region, 141980, Russian Federation
[2] Dubna State University, Dubna, Moscow Region, 141980, Russian Federation
[3] Umarov Physical Technical Institute, TAS, Dushanbe, 734063 Tajikistan
[4] Department of Physics, University of South Africa, Florida 1710, South Africa
[5] Department of Experimental Physics, Comenius University, Bratislava, Slovakia
[6] Friedrich-Schiller-Universität, Institut für Festkörperphysik, Jena, D-07743 Jena, Germany
[7] Poznan University of Technology, Poznan, Poland

E-mail: shukrinv@theor.jinr.ru

Received 13 September 2016, revised 28 October 2016
Accepted for publication 10 November 2016
Published 14 December 2016

Abstract

Resonance phenomena in a model of intrinsic Josephson junctions shunted by *LC*-elements (*L*-inductance, *C*-capacitance) are studied. The phase dynamics and *IV*-characteristics are investigated in detail when the Josephson frequency approaches the frequency of the resonance circuit. A realization of parametric resonance through the excitation of a longitudinal plasma wave, within the bias current interval corresponding to the resonance circuit branch, is demonstrated. It is found that the temporal dependence of the total voltage of the stack, and the voltage measured across the shunt capacitor, reflect the charging of superconducting layers, a phenomenon which might be useful as a means of detecting such charging experimentally. Thus, based on the voltage dynamics, a novel method for the determination of charging in the superconducting layers of coupled Josephson junctions is proposed. A demonstration and discussion of the influence of external electromagnetic radiation on the *IV*-characteristics and charge-time dependence is given. Over certain parameter ranges the radiation causes an interesting new type of temporal splitting in the charge-time oscillations within the superconducting layers.

Keywords: intrinsic Josephson junctions, shunting, resonance feature, charging, modelling

(Some figures may appear in colour only in the online journal)

1. Introduction

The Josephson effect is a powerful instrument for the investigation of high temperature superconductivity materials such as $Bi_2Sr_2CaCu_2O_8$, where the superconducting layers form intrinsic Josephson junctions (IJJs) [1]. Since the thickness of the superconducting layer (S-layer) in the IJJs is comparable to the Debye screening length, the S-layers are in the nonstationary, nonequilibrium state, due to the injection of quasiparticles and Cooper pairs [2, 3]. The charge neutrality in the S-layers is locally broken and this charging effect modifies the Josephson equation that relates the voltage to the rate of change in the phase difference. Questions relating to the value of the electric charge in the S-layers, and particularly its maximum value at the parametric resonance, have not yet been investigated experimentally. Koyama and Tachiki [2] demonstrated that the system of equations for capacitively coupled Josephson junctions has a solution corresponding to a longitudinal plasma wave (LPW) propagating along the *c*-axis. The Josephson oscillations can excite this LPW by their periodic actions [4]. The frequency of the Josephson oscillations ω_J is determined by the junction voltage, and the parametric resonance is realized when $\omega_J = 2\omega_{LPW}$, where ω_{LPW} is LPW frequency. This means that there is a resonance point at which a LPW with a definite wave number is created in the stack of junctions.

Shunting of Josephson junctions by inductive and capacitive circuit elements (so-called *LC*-shunting), forms an

multiple resonance circuit. Such shunting allows effective control and manipulation of the resonance features, which are potentially useful in superconducting electronics. When the Josephson frequency ω_J equal to the resonance frequency of the circuit ω_{rc}, the oscillations in Josephson junction are tuned to this frequency. This resonance could manifested itself in the current–voltage characteristic (*IV*-characteristic) in a variety of ways; such as, steps [5, 6], or humps and dips [7, 8]. *LC*-shunting leads to a step in the one loop *IV*-characteristics, when the value of Josephson frequency approaches that of the resonance circuit. As we have discussed previously, the location of this step depends on parameters of the *LC*-circuit [9]. The existence of steps in the *IV*-characteristic of various shunted systems of Josephson junctions has also been reported in a number of experimental and theoretical works. (See, for example, [10, 11].)

In [9] the possibility of the appearance of an additional parametric resonance, owing to the resonance circuit formed in the system of coupled Josephson junctions with *LC*-shunting, has been demonstrated. As expected, in this case also, a LPW of half the Josephson frequency is excited. The resonance between the Josephson oscillations and those of the *LC*-circuit triggers the fundamental parametric resonance, which is sustained throughout the region over which there is a transition to inner branches of the *IV*-characteristic.

A strong *LC*-shunting effect on the *IV*-characteristic and voltage–time dependence of Josephson junction under external electromagnetic radiation was also demonstrated in [12, 13]. Crucial changes were found at the resonance condition when the radiation frequency coincided with the Josephson and resonance circuit frequencies, demonstrating a change in the amplitude dependence of the Shapiro step width. Shunting of the junctions provides an extended range of Bessel behavior. For the same microwave source, the Shapiro steps follow the usual Bessel behavior at much smaller radiation power, in comparison to the unshunted case. Such new features of the Shapiro step on the resonance branch are of interest to quantum metrology [14].

In this paper we first present results on the modeling of a shunted single JJ as an example of a Josephson nanostructure. We then describe the novel features that appear in our shunted system of coupled JJs, which is a model for IJJs in high-T_c superconductors. We concentrate on the properties of parallel resonance realized at the conditions when the Josephson frequency approaches the frequency of the resonance circuit formed by the IJJs with *LC*-shunting. We then demonstrate the parametric resonance and excitation of a LPW over a current interval corresponding to the resonance circuit branch (*rc*-branch). We show that the temporal dependence of the total voltage across the stack (or the shunt capacitor), can reveal whether or not the superconducting layers become charged, which might be a useful criteria for observing such charging. Under the application of external electromagnetic radiation we demonstrate, by looking at the charge–time dependence, that there is an interesting temporal splitting of the charge oscillations within the superconducting layers. To the best of our knowledge, as we discuss here, this effect has not been observed in previous simulations.

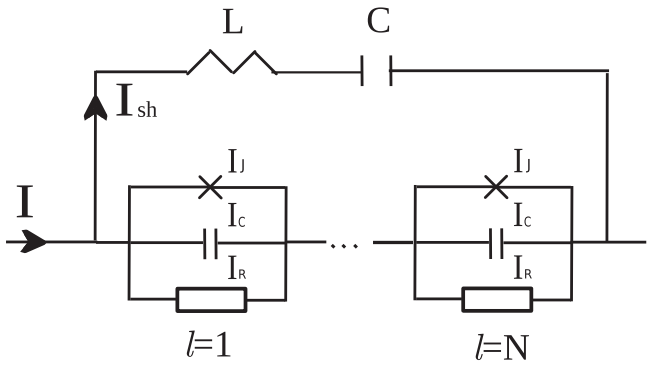

Figure 1. Schematic representation of N Josephson junctions in series, with *LC*-shunting. Each junction is represented by the well known RCSJ model, with additional capacitative coupling between adjacent RCSJ junctions, as would occur for intrinsic JJs. Thus the series stack of junctions is considered within the framework of the so-called CCJJ+DC model [9], which emerges as the first two of equations (1), by setting $C = 0$. For a single junction ($N = 1$, $\alpha = 0$) the CCJJ+DC model reduces to the RCSJ model.

One may ask what information comes out of the novel method for the detection of S-layer charging? What, beside the general test of charging, can be useful when one determines the charging values? Can it be used in some application or is it only a basic physics aspect? The answers to these questions have many aspects. We stress here the main point—a creation of LPW in the stack of coupled Josephson junctions. It is important for different related phenomena in physics and applications. Particularly, an effect of LPW on the coherent electromagnetic radiation in the terahertz frequency region is not investigated clearly yet. But obviously, it should have an effect on the radiation power. The charging of S-layers and the effect of LPWs with different parameters might also be important for electronics of nanosystems based on IJJs [15–18]. We note here another interesting feature, related to the fact that charging will require some time and thus a high charge means a longer time. This question was not touched yet in the previous investigations. The *LC* shunt can influence this time that means the speed of junction response. So, control of the charging process by an artificial optimized shunt offers new ways to control the behavior and the parameters of IJJs (especially, at high frequencies) which offers new possibilities for applications.

2. Models and methods

Consider the circuit presented in figure 1. In dimensionless form the equations describing this circuit can be written as [9]

$$\left.\begin{aligned}
&\frac{\partial\varphi_l}{\partial t} = V_l - \alpha(V_{l+1} + V_{l-1} - 2V_l),\\
&\frac{\partial V_l}{\partial t} = I + I_l^{\mathrm{n}} + A\sin(\omega_R t) - \sin\varphi_l - \beta\frac{\partial\varphi_l}{\partial t} - C\frac{\partial u_c}{\partial t},\\
&\frac{\partial^2 u_c}{\partial t^2} = \frac{1}{LC}\left(\sum_{l=1}^{N} V_l - u_c\right).
\end{aligned}\right\} \quad (1)$$

Here u_c is the voltage across the shunt capacitance C. The bias current I and added noise currents I_l^n are normalized to the critical current I_c of each JJ. A and ω_R are the amplitude and angular frequency of external electromagnetic radiation. Time is normalized to the inverse of the plasma frequency $\omega_p = \sqrt{2eI_c/(C_j\hbar)}$, the voltages V_l and u_c to $V_0 = \hbar\omega_p/(2e)$, the shunt capacitance C to the capacitance C_j of the JJ, and the shunt inductance L to $(C_j\omega_p^2)^{-1}$. In equation (1) we denote the dissipation parameter $\beta = \sqrt{\hbar/(2eI_cC_jR_j^2)} = 1/\sqrt{\beta_c}$, where β_c is McCumber's parameter. Unless explicitly stated, the added noise currents in the present simulations are drawn from a uniform distribution over the range $[-10^{-8}, +10^{-8}]$.

We note that the shunted system forms a parallel resonance circuit with the resonance frequency

$$\omega_{rc} = \sqrt{\frac{1+NC}{LC}}, \tag{2}$$

where N is the number of JJs in the stack. Furthermore, the electric charge density in the superconducting layers is determined by the difference between the voltages V_l and V_{l+1} across the neighboring insulating layers [19, 20], i.e.

$$Q_l = Q_0\alpha(V_{l+1} - V_l), \tag{3}$$

where $Q_0 = \varepsilon_r\varepsilon_0V_0/r_D^2$, ε_r is the relative permittivity and ε_0 is the permittivity of free space. For brevity we will refer to Q simply as the charge.

In the results that follow, we have normalized Q to Q_0. For typical values: $r_D = 3 \times 10^{-10}$ m, $\varepsilon_r = 25$, and $\omega_p = 10^{12}$ s^{-1}, we find $V_0 = 3 \times 10^{-4}$ V and $Q_0 = 8 \times 10^5$ Cm^{-3}. Thus, for a superconducting layer with area $S = 1\ \mu$m^2 and thickness $d_s = 3 \times 10^{-10}$ m, the charge value is about 2.4×10^{-16} C. This value of charge is sufficiently high to play a significant role in the physical processes in the stack of IJJs in high temperature superconductors.

3. The *rc*-branch features of a single JJ

Resonance circuit branches (*rc*-branches) in *IV*-characteristics are a manifestation of the parallel resonance in the shunted system. They correspond to the stable side of the resonance peak. Since the other peak side has a negative slope, it is unstable and it is not manifested in *IV*-characteristic [10]. The form of the obtained resonance branch depends on the values of L and C. It usually has a gentle slope on a graph of V against I. Changes in the parameter values for the JJ and resonance circuit can influence the slope [9], as we see in figure 2.

Figure 2 shows two cycle *IV*-characteristic for a single JJ with *LC*-shunting with large and small shunt capacitance. In both cases depicted in figure 2, the circuit resonance frequency was the same, corresponding to the average total voltage $V = 3$. We see that *rc*-branch at small C has practically no slope. This is because the slope characterizes the width of the parallel resonance peak, and changing in quality factor $F = R_j\sqrt{\frac{C}{L}}$ of the parallel resonance also changes the width of the peak, and consequently the slope of *rc*-branch.

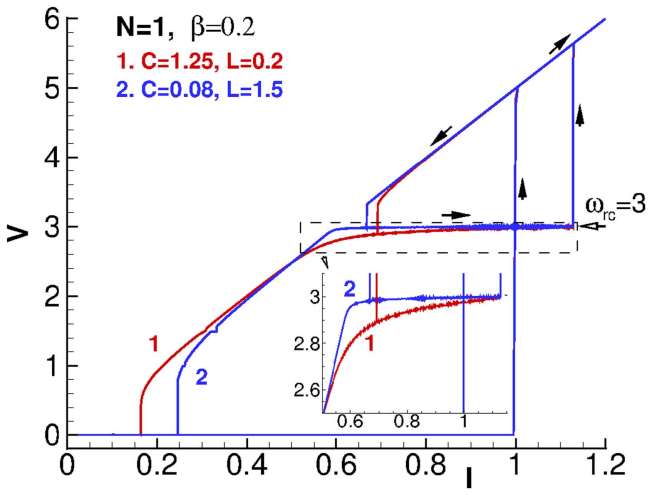

Figure 2. Two cycle *IV*-characteristics for a single JJ with *LC*-shunting. Curve 1 is for a large shunt capacitance ($C = 1.25$), while curve 2 is for a much smaller shunt capacitance ($C = 0.08$). The current cycle used to obtain both *IV*-characteristics was $0 \longrightarrow 1.2 \longrightarrow 0.5 \longrightarrow 1.2 \longrightarrow 0$ and the inductances we chosen to give a constant value of $\omega_{rc} = 3$, in equation (2). The inset shows the different slopes of the two resonance branches.

Manifestation of parallel and series resonances in shunted Josephson junctions can be seen clearly in the temporal dependence of the total voltage $V(t)$. Figure 3 presents the temporal dependence of the voltage together with corresponding part of *IV*-characteristic, including *rc*-branch, calculated at different C and L with increasing in a bias current along the *rc*-branch. Figure 3(a) show the result for $L = 45$, $C = 0.002$ (small capacitance), where we see a disappearance of voltage oscillations around point A, which corresponds to the series circuit resonance frequency $\omega = 1/\sqrt{LC}$, and a maximum voltage amplitude at the point B, related to the parallel circuit resonance. Figure 3(b) shows the same features for the case of a much larger shunt capacitance.

4. Double resonance in the system of coupled JJs

The direct experimental observation of the electric charge in superconducting layers is a very difficult task due to its small value and the extreme thinness of superconducting layers [19–21]. Here we show that the temporal dependence of the total voltage across the stack, and correspondingly, the temporal dependence of the voltage across the shunt capacitor, reflect the charging that occurs in the superconducting layers. The resonance of the Josephson oscillations, with those of the *LC*-circuit, acts as a trigger for an additional parametric resonance in the system of coupled Josephson junctions with *LC* shunting. This leads to the charging of S-layers in the stack and excitation of a LPW with a frequency of half the Josephson frequency [9].

Figure 4 presents the temporal dependence of the charge on the shunt capacitor (light, blue) and in an S-layer (dark, orange) together with corresponding part of *IV*-characteristic including the *rc*-branch. Calculations have done for the

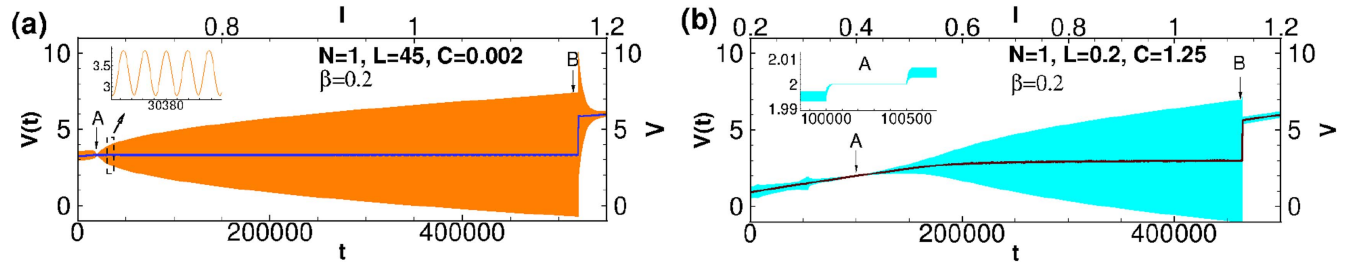

Figure 3. Temporal dependence of the total voltage as a function of increasing bias current, for the *rc*-branch of the *IV*-characteristic (time averaged voltage is shown by a dark solid line). Letters *A* and *B* indicate the position of series and parallel resonances in the system, respectively. In (a), $L = 45$, $C = 0.002$; while in (b), $L = 0.2$, $C = 1.25$.

system of ten JJs shunted by $C = 0.002$ and three different values of inductance. As it is demonstrated in figure 4(a), the electric charge in S-layers at $L = 42$ is absent. The charge in the capacitor is simulated with an increase in bias current and we see the monotonic increase of the amplitude of charge oscillations up to the resonance point $\omega_J = \omega_{rc}$.

The charge in S-layers appears and grow with an increase in L. At $L = 45$ ($\omega_{rc} = 3.367$), as we see in figure 4(b), the charge in S-layer exists simultaneously with the charge in the capacitor. We note the changes in the monotonic increase of the charge oscillation amplitude in the interval marked by dashed lines. We see some range of reduced amplitude in the temporal dependence of the capacitor charge. Very clear this range of reduced amplitude is demonstrated in figure 4(c) at $L = 48$. Analysis of the charge distribution along the stack shows that a LPW with $\lambda = 2d$ is realized, where d is a period of the stack. Figure 4(d) shows the voltage dynamics in the stack in compare with figure 4(c). The inset shows the LPW with wave length $\lambda = 2$ which is realized in the stack at $I = 0.85$. The dashed lines actually indicate the bias current interval where LPW exists along the stack. Decrease in ω_{rc} leads to the growth of this current interval. Now, for $\omega_{rc} = 3.2596$, the charge in S-layers can be registered along one loop *IV*-characteristic after a jump to the resonance branch from the outermost branch with a decrease in bias current.

As follows from the third equation in the system (1), the charge in the shunt capacitor is

$$Q_c = \frac{u_c}{C} = \frac{1}{C}\left(\sum_{l=1}^{N} V_l - LC\frac{\partial^2 u_c}{\partial t^2}\right). \qquad (4)$$

The decrease of the shunt capacitor oscillation amplitude is related to the decrease of the difference in the bracket of equation (4). Furthermore, from equation (3) it is clear that a growth in charge in the S-layers is accompanied by an increasing phase shift between V_l and V_{l+1}.

The result presented in figure 4(c) has been repeated for the cases without added noise (figure 5(a)) and with added noise (figure 5(b)). Without any added noise in the numerical simulation no charging occurs within the layers over any part of the cycle. As the current is reduced, we follow the outer (upper) branch of the *IV*-characteristic, starting from the blue arrow in figure 5(a). V is the time average of the total voltage oscillation, $V(t)$. As shown by the green dashed line, the amplitude of $V(t)$ gradually increases, relative to its average, from about 1.75 to 3.75, i.e. starting from the green arrow and following the lower dashed line in the direction of the arrow. At $I \approx 0.72$ there is a sharp resonance between ω_{rc} and the Josephson frequency, causing a rapid increase in the amplitude of $V(t)$, as we jump from the outer branch of the *IV*-characteristic onto *rc*-branch. The system then remains in resonance for the rest of the current cycle. As the current increases from 0.7 $\longrightarrow$ 1.2 the amplitude of $V(t)$ increases to a maximum value of about 41, before the resonance is lost and the system returns to the outer branch. It is important to note that, throughout the current cycle, the oscillations in all the junctions remain synchronized, for the case in (a).

As noted in earlier work, the added noise simulates thermal fluctuations that may occur in real systems, and which act as a catalyst for the onset of parametric resonance [4]. Thus in figure 5(b), although the same current cycle as in (a) is performed, there is now an additional parametric resonance due to the excitation of a LPW within the stack of junctions. The creation of this LPW is accompanied by a desynchronization between the junctions. This desynchronization may be clearly observed, not only in the increase of the maximum charge amplitude, but also in a decrease of the total voltage amplitude, as the voltage signals from the different junctions no longer add in phase. In figure 5(b) we see that there are now effectively two slopes in the resonating part of the $V(t)$ amplitude. One characterizes the rate at which the amplitude increases with charging, the other (smaller value), the rate without. In figure 5(b) it can be seen that the LPW, giving rise to the non-zero charge amplitude, is sustained up to a current of $I \approx 0.93$ on the return part of the cycle.

When the circuit resonance frequency, ω_{rc}, is close enough to the fundamental parametric resonance, the behavior of charge oscillations are essentially changed [9]. The charging of the superconducting layers is demonstrated very clearly in figure 6 where we show the charge–time dependence in the first S-layer of ten Josephson junctions at $C = 0.002$, $L = 55$. Increase in L in compare with results presented in figure 4, decrease the ω_{rc} and approaches it to the frequency of fundamental parametric resonance. Dashed rectangles in figure 6(a) marked two regions with different character of charge oscillations. Figure 6(c) demonstrate enlarged region B where the character of the charge oscillations is the same as we saw in figures 4(b), (c). On the other hand the oscillations in region A (figure 6(b)) exhibit amplitude modulations.

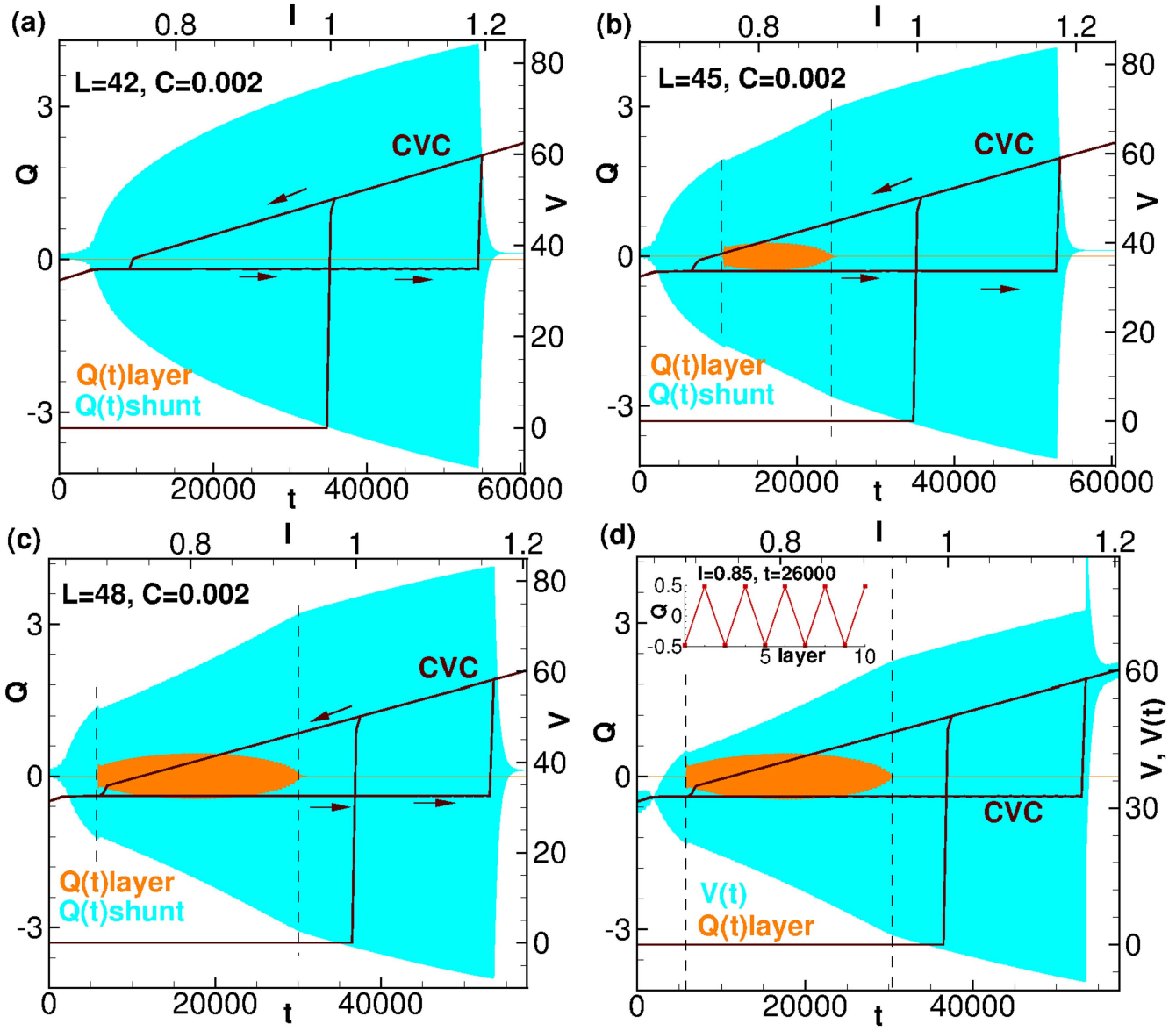

Figure 4. Temporal dependence of the charge on shunted capacitor (light, blue) and the charge in S-layers (dark, orange) together with corresponding part of *IV*-characteristic (CVC) including the *rc*-branch, calculated for the system of ten JJs shunted by $C = 0.002$, (a) $L = 42$, (b) $L = 45$, (c) $L = 48$. (d) Voltage–time dependence and charge–time dependence with the corresponding part of the *IV*-characteristic of the system of $N = 10$ JJ shunted by resonant circuit with $\omega_{rc} = 3.2596$ (L and C the same as in (c)). The inset shows the longitudinal plasma wave with wave length $\lambda = 2$ which exists in the stack at $I = 0.85$.

It is known that the superconducting circuit consisting of Josephson junctions coupled to a cavity represents an example of a birhythmic system. The two states at fixed value of biased current are clearly characterized by two different frequencies. The coexistence of two attractors leads to the fact that, in the presence of noise, the system can switch from one attractor to the other [22]. The origin of the observed modulation is probably related to the manifestation of birhythmicity in the system. The region A corresponds to the current interval where the outermost and resonance circuit branch (*rc*-branch) are close together, so this region is most sensitive to the additional perturbations. Additionally, we stress that with an increase in L the frequency of the parallel resonance $\omega_{rc} = \sqrt{(1 + NC)/(LC)}$ is decreased, approaching the parametric resonance in the system, realized in the linear stack of coupled Josephson junctions [4, 21, 23]. So, conditions for more complex resonance are getting possible. The features of this phenomena for stack of coupled JJs will be described in detailed somewhere else.

5. Effect of radiation

In this section we consider our system under external electromagnetic radiation. Figure 7 shows the *IV*-characteristic and charge–time dependence for the first S-layer of ten JJs at frequency of radiation $\omega_R = 3.2596$, equal to the frequency of the resonance circuit, and amplitude $A = 0.2$.

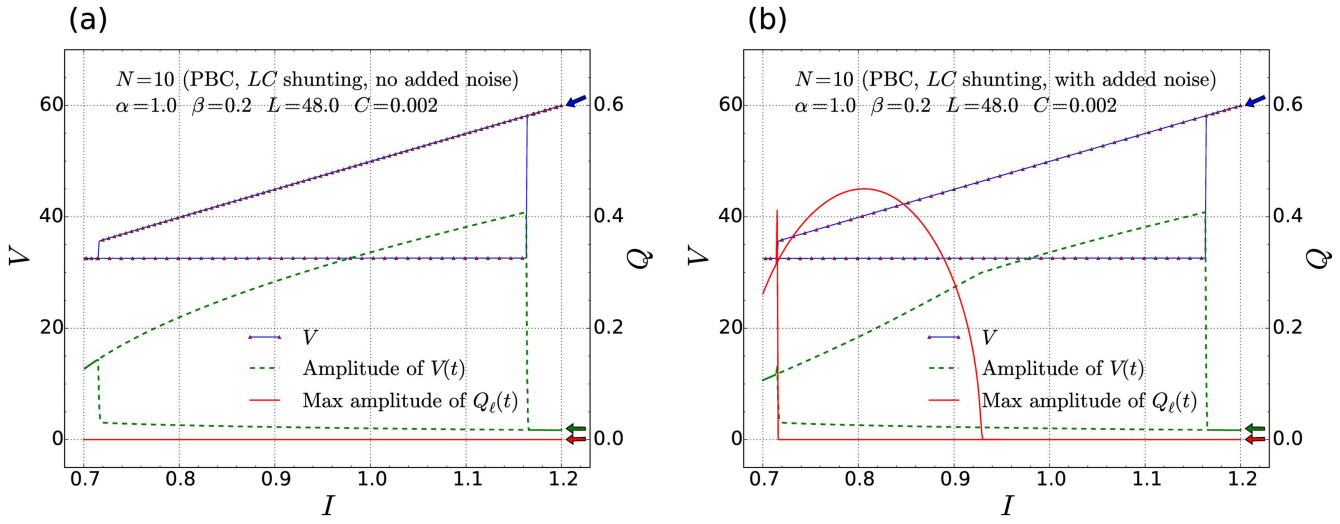

Figure 5. Manifestation of S-layer charging by changing amplitude of voltage oscillations. (a) Part of *IV*-characteristic and maximal voltage amplitude without added noise. (b) The same as in (a) with added noise. In both figures one current cycle is performed: $1.2 \longrightarrow 0.7 \longrightarrow 1.2$. The starting value ($I = 1.2$) and initial direction of the current cycle (decreasing current) is indicated by the arrows, to the right of the figure.

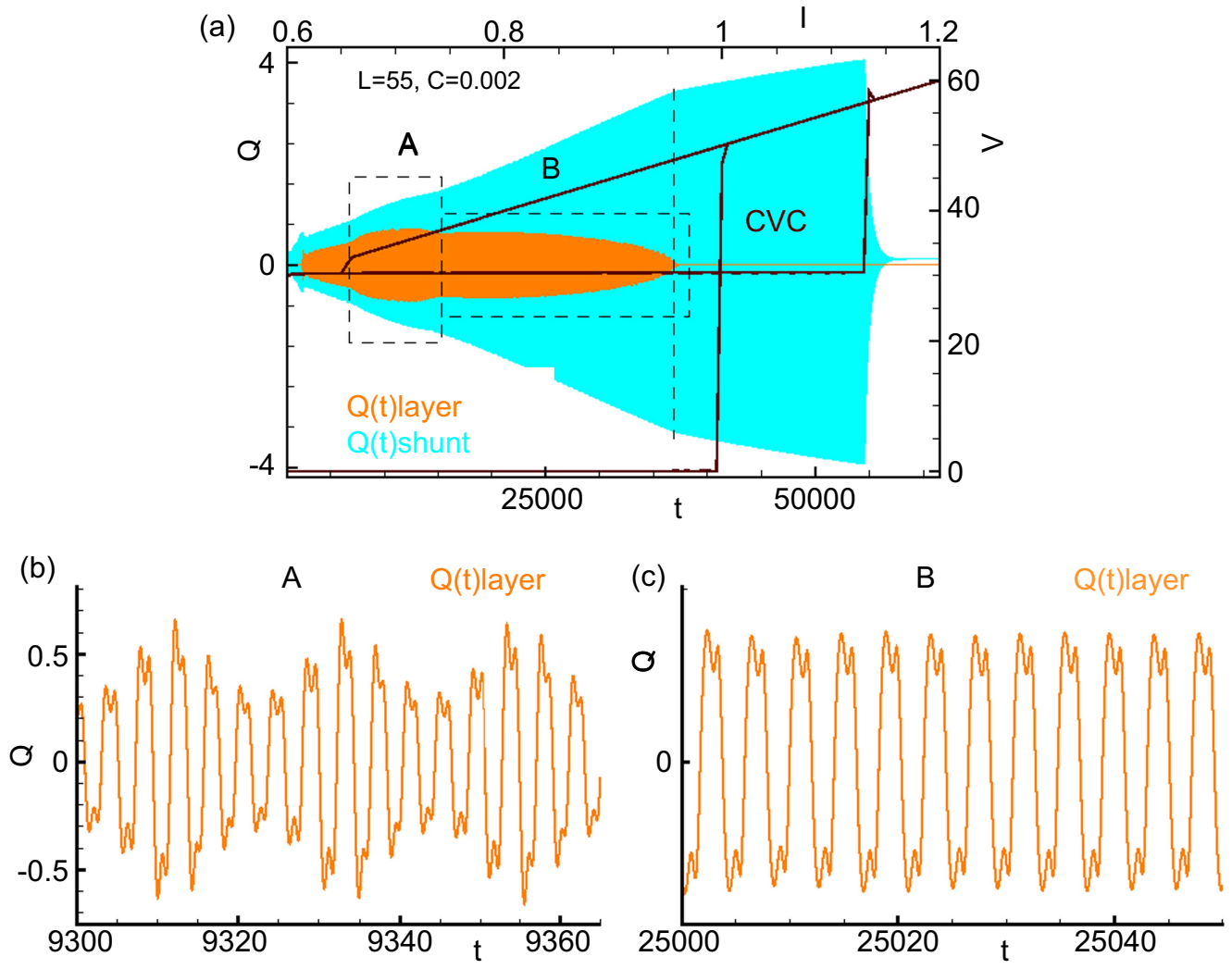

Figure 6. (a) Temporal dependence of the charge on shunted capacitance (light, blue) and in S-layers (dark, orange) together with corresponding part of *IV*-characteristic (CVC) including *rc*-branch, calculated for the system of $N = 10$ JJs shunted by $C = 0.002$, $L = 55$; (b) character of oscillations in region *A*; (c) character of oscillations in region *B*.

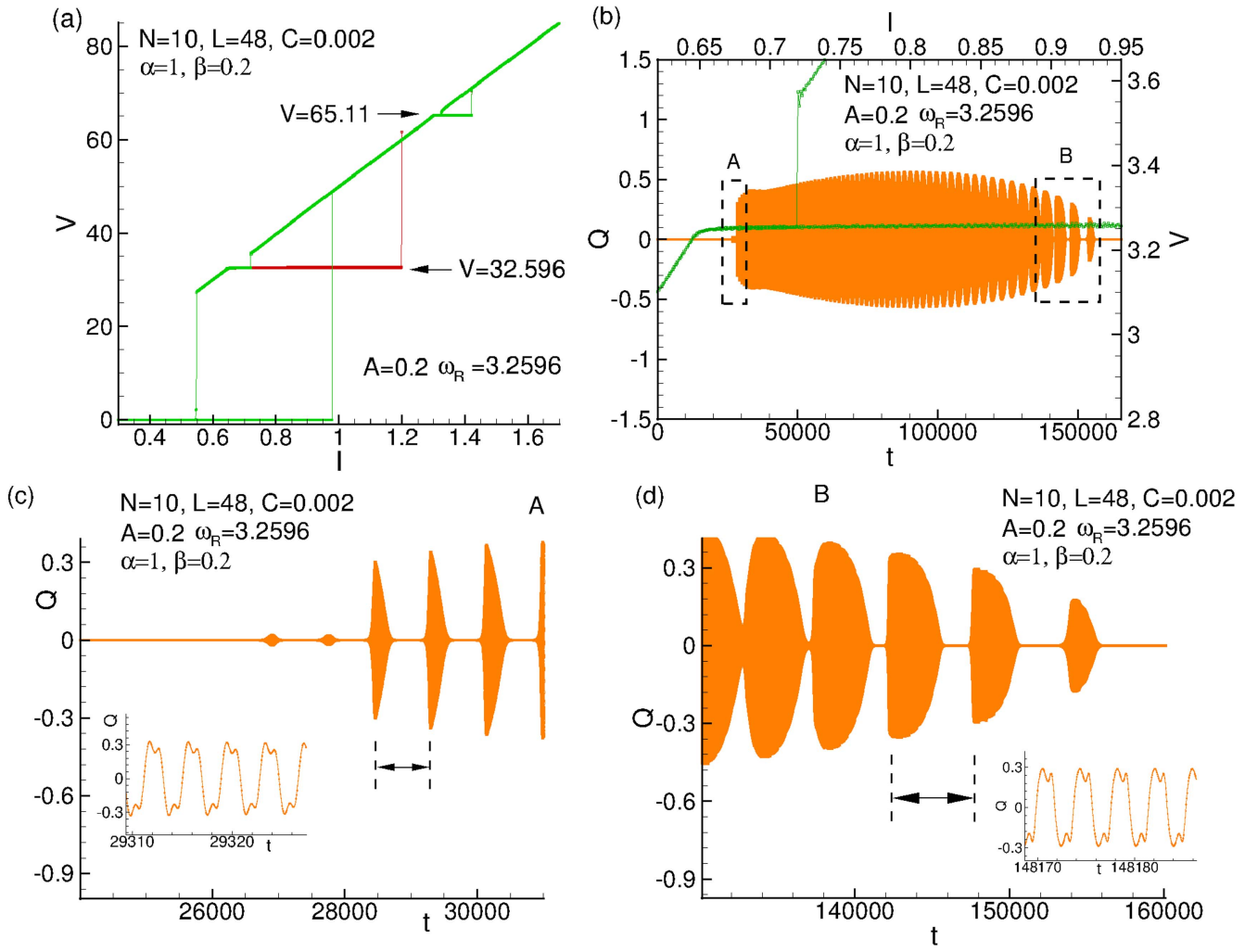

Figure 7. (a) *IV*-characteristic of the system of ten JJs at $\beta = 0.2$, $\alpha = 1$, $L = 48$ and $C = 0.002$ under external electromagnetic radiation with frequency $\omega_R = 3.2596$ and amplitude $A = 0.2$. (b) Charge–time dependence for the first superconducting layer in the stack at the same parameters as in (a). (c) and (d) Enlarged parts of charge–time dependence in the beginning and at the end of the charging interval, respectively. Insets demonstrate character of charge oscillations in the corresponding regions.

The *IV*-characteristic (figure 7(a)) has the Shapiro step at the end of the *rc*-branch (at $V = 32.596$ and its harmonic at $V = 65.110$), so the charging interval does not touch it. Charging of superconducting layers (shown in figure 7(b)) appears in the current interval corresponding to the central part of *rc*-branch which is lower than a position of the Shapiro step on voltage scale. Below we will discuss the features in the case when charging happens in the current interval, overlapped with a Shapiro step. In the present case, as we have seen in this figure, we have observed a splitting of charge oscillations in the superconducting layers for some time regions.

Figures 7(c), (d) enlarge the dependence at the onset and at the end of the charging interval, demonstrating the splitting character of the charge oscillations. We see that the time interval (period) of splitting increases as the resonance point is approached, but the character of oscillations, shown in the inset to the figures, does not change. The observed splitting is a manifestation of a beating of Josephson and radiation frequencies with a period $T_m = \frac{2\pi}{|\omega_J - \omega_R|}$. So, we expect that temporal splitting of charge oscillations would disappear in the bias current interval corresponded to the overlapping of charging interval in current and the Shapiro step. This feature is demonstrated in figure 8.

Splitting of the charge oscillation is observed in the case when the width of the Shapiro step is smaller than the charging interval (see figure 8(a)). It disappears completely at larger amplitude of the external radiation, when the charging interval and width of the Shapiro step are of the same size and they are overlap, as we can see in figure 8(b).

6. Conclusions

We have studied the resonance phenomena in Josephson junctions shunted by *LC*-circuit elements. Our model includes coupling which is appropriate for IJJs that occur in certain high-T_c superconductors. The phase dynamics and *IV*-

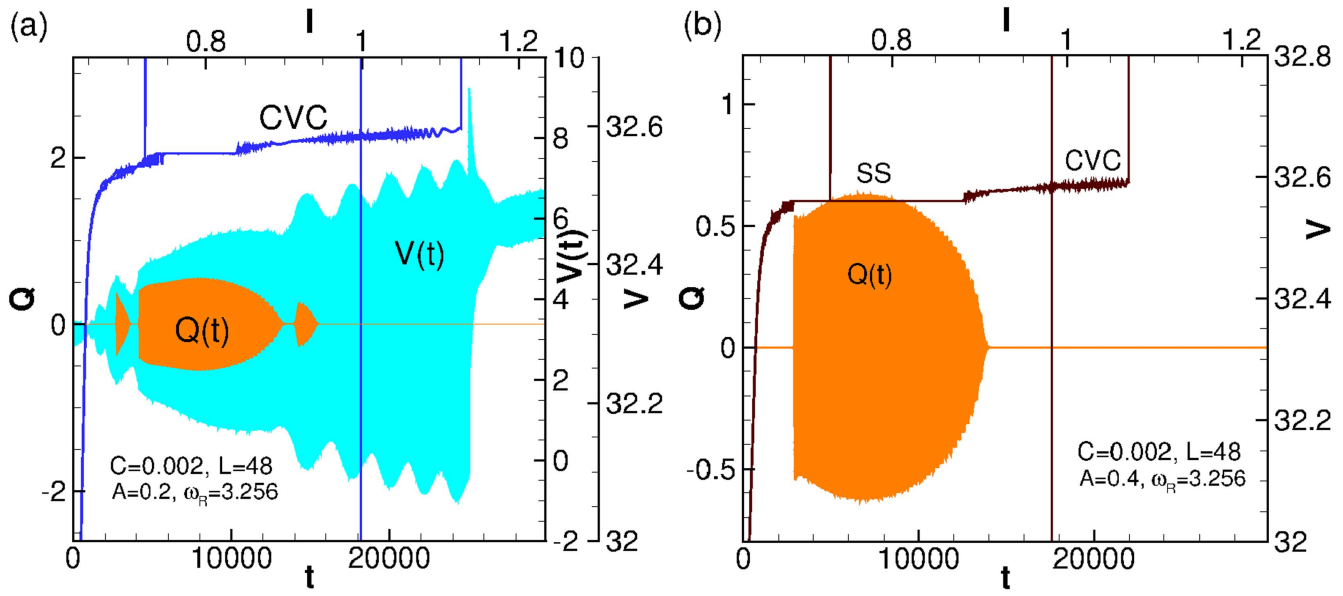

Figure 8. (a) Charge–time $Q(t)$ (for first S-layer) and voltage–time $V(t)$ (for first JJ in the stack) dependencies with the corresponding part of the *IV*-characteristic (CVC) of the system of $N = 10$ JJ shunted by resonant circuit with $\omega_{rc} = 3.2596$ under electromagnetic radiation with frequency $\omega_R = 3.256$ and amplitude $A = 0.2$. *V*-axis indicate the total average voltage of the stack; (b) $Q(t)$ together with *IV*-characteristic at the same frequency and $A = 0.4$.

characteristics were investigated in detail as the Josephson frequency approaches the circuit resonance circuit frequency. A realization of parametric resonance and excitation of LPW in the current interval corresponding to the resonance circuit branch was demonstrated. We found that the temporal dependence of the shunt capacitance voltage (or that of the total voltage) reflects the charging of S-layers. Based on this result, we proposed a novel method for detecting charging in the present systems of coupled Josephson junctions with *LC*-shunting. The influence of the external electromagnetic radiation on the *IV*-characteristics and charge–time dependence demonstrates an new effect of temporal splitting in the charge oscillations that occur within the S-layers.

Acknowledgments

We thank E Ilichev and M Grajcar for detailed discussion of this paper. The reported study was funded by RFBR according to the research projects 15–51–61011 – Egypt, 15–29–01217 and 16–52–45011_India. The work was supported by the Heisenberg–Landau program, Bogoliubov–Infeld program, the JINR-Slovakia and JINR-Romania collaboration. We thank W Kleinig, S Dubnichka and W Chmielovski for this support. AEB gratefully acknowledges funding for this work from Unisa's CSET research fund.

References

[1] Welp U, Kadowaki K and Kleiner R 2013 *Nat. Photon.* **7** 702
[2] Koyama T and Tachiki M 1996 *Phys. Rev.* B **54** 16183
[3] Ryndyk D A 1998 *Phys. Rev. Lett.* **80** 3376
[4] Shukrinov Y M and Mahfouzi F 2007 *Supercond. Sci. Technol.* **19** S38
[5] Jensen H D, Larsen A and Mygind J 1990 *Physica* B **165** 1661
[6] Larsen A, Jensen H D and Mygind J 1991 *Phys. Rev.* B **43** 10179
[7] Tachiki M, Ivanovic K, Kadowaki K and Koyama T 2011 *Phys. Rev.* B **83** 014508
[8] Zhou T, Mao J, Cui H, Zhao X, Fang L and Yan S 2009 *Physica* C **469** 785
[9] Shukrinov Y M, Rahmonov I R and Kulikov K V 2012 *JETP Lett.* **96** 657
[10] Likharev K K 1986 *Dynamics of Josephson Junctions and Circuits* (New York: Gordon and Breach)
[11] Almaas E and Stroud D 2002 *Phys. Rev.* B **65** 134502
[12] Shukrinov Y M, Rahmonov I R, Kulikov K V and Seidel P 2015 *Europhys. Lett.* **110** 47001
[13] Kornev V K and Kolotinskiy N V 2016 *IEEE Trans. Appl. Supercond.* **26** 1601605
[14] Jeanneret B and Benz S P 2009 *Eur. Phys. J. Spec. Top.* **172** 181
[15] Rudau F *et al* 2016 *Phys. Rev. Appl.* **5** 044017
[16] Zhou X J *et al* 2015 *Phys. Rev. Appl.* **3** 044012
[17] Delfanazari K, Asai H, Tsujimoto M, Kashiwagi T, Kitamura T, Yamamoto T, Wilson W, Klemm R A, Hattori T and Kadowaki K 2015 *IEEE Trans. Terahertz Sci. Technol.* **5** 505
[18] Zhou X *et al* 2015 *Appl. Phys. Lett.* **107** 122602
[19] Shukrinov Y M and Gaafar M A 2011 *Phys. Rev.* B **84** 094514
[20] Shukrinov Y M, Mahfouzi F and Suzuki M 2008 *Phys. Rev.* B **78** 134521
[21] Shukrinov Y M and Mahfouzi F 2007 *Phys. Rev. Lett.* **98** 157001
[22] Yamapi R and Filatrella G 2014 *Phys. Rev.* E **89** 052905
[23] Shukrinov Y M, Mahfouzi F and Pedersen N F 2007 *Phys. Rev.* B **75** 104508